ARTICLE

Ritanserin blocks Ca$_V$1.2 channels in rat artery smooth muscles: electrophysiological, functional, and computational studies

Fabio Fusi[1], Alfonso Trezza[1], Giampietro Sgaragli[2], Ottavia Spiga[1], Simona Saponara[2] and Sergio Bova[3]

Ca$_V$1.2 channel blockers or 5-HT$_2$ receptor antagonists constitute effective therapy for Raynaud's syndrome. A functional link between the inhibition of 5-HT$_2$ receptors and Ca$_V$1.2 channel blockade in arterial smooth muscles has been hypothesized. Therefore, the effects of ritanserin, a nonselective 5-HT$_2$ receptor antagonist, on vascular Ca$_V$1.2 channels were investigated through electrophysiological, functional, and computational studies. Ritanserin blocked Ca$_V$1.2 channel currents ($I_{Ca1.2}$) in a concentration-dependent manner ($K_r = 3.61$ μM); $I_{Ca1.2}$ inhibition was antagonized by Bay K 8644 and partially reverted upon washout. Conversely, the ritanserin analog ketanserin (100 μM) inhibited $I_{Ca1.2}$ by ~50%. Ritanserin concentration-dependently shifted the voltage dependence of the steady-state inactivation curve to more negative potentials ($K_i = 1.58$ μM) without affecting the slope of inactivation and the activation curve, and decreased $I_{Ca1.2}$ progressively during repetitive (1 Hz) step depolarizations (use-dependent block). The addition of ritanserin caused the contraction of single myocytes not yet dialyzed with the conventional method. Furthermore, in depolarized rings, ritanserin, and to a lesser extent, ketanserin, caused a concentration-dependent relaxation, which was antagonized by Bay K 8644. Ritanserin and ketanserin were docked at a region of the Ca$_V$1.2 α$_{1C}$ subunit nearby that of Bay K 8644; however, only ritanserin and Bay K 8644 formed a hydrogen bond with key residue Tyr-1489. In conclusion, ritanserin caused in vitro vasodilation, accomplished through the blockade of Ca$_V$1.2 channels, which was achieved preferentially in the inactivated and/or resting state of the channel. This novel activity encourages the development of ritanserin derivatives for their potential use in the treatment of Raynaud's syndrome.

Keywords: ritanserin; Ca$_V$1.2 channel; Raynaud's syndrome; 5-HT$_2$ receptor; docking simulation; homology modeling

INTRODUCTION

Ritanserin (6-[2-[4-[*bis*(4-fluorophenyl)methylidene]piperidin-1-yl]ethyl]-7-methyl-[1,3]thiazolo[3,2-a]pyrimidin-5-one) is a potent, long acting, nonselective 5-HT$_2$ receptor antagonist [1, 2] and is classified as an antidepressant agent [3], although it has never been approved for clinical use. It has an additional intrinsic antidopaminergic effect, possibly underlying the reported improvement of negative symptoms in patients who have schizophrenia [4]. Moreover, a number of preclinical and clinical studies have examined the effectiveness of ritanserin at reducing cocaine cravings and/or cocaine use [5].

The direct action of ritanserin on Na$^+$ and Ca^{2+} channels has been shown in canine Purkinje fibers, where it produces significant depressant effects on transmembrane action potentials [6], which are credited for its antiarrhythmic activity.

Recently, evidence that ritanserin inhibits several lipids (e.g., diacylglycerol kinase-α, DGKα, a novel, potential therapeutic target in various cancers as well as in immunotherapy) [7–9] and protein kinases (e.g., the feline encephalitis virus-related kinase FER) [10], as well as the rapidly accelerated fibrosarcoma kinase c-RAF [11] has been provided. The capacity of perturbing cellular signaling pathways important for cell survival and proliferation, through serotonin-independent mechanisms suggests that ritanserin may be a viable option for in vivo translation and a novel therapeutic tool with potential applications in various tumors.

The serotoninergic antagonism of ritanserin, characterized by a long duration of action, has been shown in a variety of peripheral cardiovascular, gastrointestinal, and respiratory vascular tissues [12]. In the rat tail artery, the interaction of ritanserin with an allosteric site near the 5-HT$_2$ receptor was presumed, owing to ritanserin antagonism of the effects of 5-HT that are different from that of another 5-HT$_2$ receptor antagonist, ketanserin (3-[2-[4-(4-fluorobenzoyl)piperidin-1-yl]ethyl]-1*H*-quinazoline-2,4-dione) [13]. Furthermore, ritanserin also antagonizes histaminergic (H$_1$) and adrenergic (α$_1$) responses in the rabbit femoral artery, though at concentrations one to three orders of magnitude higher than those needed to block 5-HT$_2$ receptors.

Several studies have demonstrated the activity of this antagonist on vascular function. In vitro as well as in vivo, ritanserin potently inhibits the 5-HT-induced vasoconstriction and pressure responses of an isolated, perfused mesenteric artery preparation [14]. Furthermore, ritanserin is also an in vitro

Ritanserin blocks the vascular Ca$_V$1.2 channel
F Fusi et al.

1159

competitive antagonist of noradrenaline and decreases the mean arterial blood pressure of anaesthetized rats.

Ketanserin fails to antagonize 5-HT-induced contractions in rat aorta rings pretreated with verapamil, a Ca$_V$1.2 channel blocker [15]. This phenomenon was explained by the direct interaction of 5-HT$_2$ receptor antagonists with the Ca$_V$1.2 channel protein [16]. Finally, similarity in the pharmacology of Ca$_V$1.2 channel blockers and 5-HT$_2$ receptor antagonists has been suggested [17]. In fact, both classes of compounds are capable of antagonizing 5-HT-induced and high K$^+$-induced contractions in rat aorta rings.

Sarpogrelate, a 5-HT$_2$ receptor antagonist registered in Japan, China, and South Korea, is used to improve vascular function in patients with peripheral artery disease and symptoms related to Raynaud's syndrome, which is characterized by reduced blood flow to the fingers and toes caused by vessel tightening or spasms in the cold [18–20]. As Ca$_V$1.2 channel blockers, such as nifedipine, have recently been confirmed as useful agents to reduce the frequency, duration, severity of attacks, pain, and disability associated with Raynaud's syndrome [21], the aim of the present study was to analyze the effect of ritanserin on the vascular Ca$_V$1.2 channel. Although the functional effects of ritanserin on blood vessels have been extensively investigated, its possible interaction with Ca$_V$1.2 channels, which are fundamental regulators of vascular muscle tone and function [22], has never been investigated. Therefore, patch-clamp, functional, and molecular-docking analyses of ritanserin effects were performed on rat tail arteries.

MATERIALS AND METHODS
Animals
All animal care and experimental protocols conformed to the European Union Guidelines for the Care and Use of Laboratory Animals (European Union Directive 2010/63/EU) and were approved by the Italian Department of Health (666/2015-PR). Male Wistar rats (250–350 g, Charles River Italia, Calco, Italy) were anaesthetized (i.p.) with a mixture of Zoletil 100® (7.5 mg·kg^{-1} tiletamine and 7.5 mg·kg^{-1} zolazepam; Virbac Srl, Milan, Italy) and Rompun® (4 mg·kg^{-1} xylazine; Bayer, Milan, Italy), decapitated and exsanguinated. The tail was isolated immediately, cleaned of skin and placed in physiological solution (namely an external solution or modified Krebs–Henseleit solution; see sections "Cell isolation procedure" and "Functional experiments", respectively). The tail main artery was dissected free of its connective tissue and cells or rings prepared as detailed in sections "Cell isolation procedure" and "Functional experiments", respectively.

Cell isolation procedure
Smooth muscle cells were freshly isolated from the tail main artery under the following conditions. A 5-mm long piece of artery was incubated at 37 °C for 40–45 min in 2 mL of 0.1 mM Ca^{2+} external solution (in mM: 130 NaCl, 5.6 KCl, 10 HEPES, 20 glucose, 1.2 MgCl$_2$, and 5 Na-pyruvate; pH 7.4) containing 20 mM taurine, which replaced an equimolar amount of NaCl, 1.35 mg·mL^{-1} collagenase (type XI), 1 mg·mL^{-1} soybean trypsin inhibitor, and 1 mg·mL^{-1} bovine serum albumin. This solution was gently bubbled with a 95% O$_2$–5% CO$_2$ gas mixture to stir the enzyme solution, as previously described [23]. Cells stored in 0.05 mM Ca^{2+} external solution containing 20 mM taurine and 0.5 mg·mL^{-1} bovine serum albumin at 4 °C under a normal atmosphere were used for experiments within 2 days after isolation [24].

Whole-cell patch clamp recordings
Cells were continuously superfused with external solution containing 0.1 mM Ca^{2+} and 30 mM tetraethylammonium (TEA) using a peristaltic pump (LKB 2132, Bromma, Sweden) at a flow rate of 400 µL·min^{-1}. The conventional whole-cell patch-clamp method was employed to voltage clamp smooth muscle cells. Recording

electrodes were pulled from borosilicate glass capillaries (WPI, Berlin, Germany) and fire-polished to obtain a pipette resistance of 2–5 MΩ when filled with internal solution. The internal solution (pCa 8.4) consisted of (in mM): 100 CsCl, 10 HEPES, 11 EGTA, 2 MgCl$_2$, 1 CaCl$_2$, 5 Na-pyruvate, 5 succinic acid, 5 oxaloacetic acid, 3 Na$_2$ATP, and 5 phosphocreatine; the pH was adjusted to 7.4 with CsOH.

An Axopatch 200B patch-clamp amplifier (Molecular Devices Corporation, Sunnyvale, CA, USA) was used to generate and apply voltage pulses to the clamped cells and record the corresponding membrane currents. At the beginning of each experiment, the junction potential between the pipette and bath solution was electronically adjusted to zero. Current signals, after compensation for whole-cell capacitance and series resistance (between 70% and 75%), were low-pass filtered at 1 kHz and digitized at 3 kHz prior to being stored on the computer hard disk. Electrophysiological responses were tested at room temperature (20–22 °C).

The $I_{Ca1.2}$ was recorded in an external solution containing 30 mM TEA and 5 mM Ca^{2+}. The current was elicited with 250 ms clamp pulses (0.067 Hz) to 10 mV from a V_h of either −50 or −80 mV. Data were collected once the current amplitude had been stabilized (usually 7–10 min after the whole-cell configuration had been obtained). Then the various experimental protocols were performed as detailed below. Under these conditions, the current, which did not run down during the following 40 min [25], was carried almost entirely by Ca$_V$1.2 channels [24, 26].

Steady-state activation curves were derived from the current–voltage relationships. Conductance (G) was calculated from the equation $G = I_{Ca1.2}/(E_m - E_{rev})$, where $I_{Ca1.2}$ is the peak current elicited by depolarizing test pulses between −50 and 20 mV from a V_h of −80 mV; E_m is the membrane potential; and E_{rev} is the reversal potential (181 mV, as estimated by the Nernst equation). G_{max} is the maximal Ca^{2+} conductance (calculated at potentials ≤20 mV). The G/G_{max} ratio was plotted against the membrane potential and fitted to the Boltzmann equation [27].

Steady-state inactivation curves were obtained using a double-pulse protocol. Once various levels of the conditioning potential had been applied for 5 s, followed by a short (5 ms) return to the V_h of −80 mV, a test pulse (250 ms) to 10 mV was delivered to evoke the current. The delay between the conditioning potential and the test pulse allowed the full or near-complete deactivation of the channels, simultaneously avoiding partial recovery from inactivation.

K$^+$ currents were blocked with 30 mM TEA in the external solution and Cs$^+$ in the internal solution. Current values were corrected for leakage and residual outward currents using 10 µM nifedipine, which completely blocked $I_{Ca1.2}$.

The osmolarity of the 30 mM TEA-containing and 5 mM Ca^{2+}-containing external solution (320 mOsmol) and that of the internal solution (290 mOsmol) were measured with an osmometer (Osmostat OM 6020, Menarini Diagnostics, Florence, Italy).

Functional experiments
The HEPES buffer system present in the cell storage medium (i.e., external solution) may alter the response of vascular smooth muscle to vasoconstricting agents such as adrenaline and angiotensin II [28]. Therefore, in the functional experiments, the rings and cells were continuously superfused at 37 °C with a modified Krebs–Henseleit, HEPES-free solution containing (in mM): 118 NaCl, 4.75 KCl, 2.5 CaCl$_2$, 1.19 MgSO$_4$, 1.19 KH$_2$PO$_4$, 25 NaHCO$_3$, and 11.5 glucose bubbled with a 95% O$_2$–5% CO$_2$ gas mixture to create a pH of 7.4. Cells were randomly selected among those, phase-dense, presenting an elongated shape (i.e., relaxed). Single-cell shortening was quantified using ImageJ by means of the Analyze/Measure plugin with the straight-line tool (ver 1.46r, NIH, http://imagej.nih.gov/ij/download.html). The length was measured in the same cell before and after drug challenge.

Two millimiter long rings, endothelium-denuded, were obtained from the tail main artery and mounted in a homemade plexiglass support for tension recording as previously described [29] with slight modifications. The endothelium was removed by gently rubbing the lumen of the rings with a very thin rough-surfaced tungsten wire. Rings were immersed in a double chambered organ bath at 37 °C filled with a modified Krebs–Henseleit solution. Contractile tension was recorded using an isometric force transducer (Ugo Basile, Comerio, Italy) connected to a digital PowerLab data acquisition system (Power-Lab 8/30; ADInstruments, Castle Hill, Australia) and analyzed by LabChart Pro version 7.3.7 for Windows software (ADInstruments). At the beginning of the experiment, a preload of 2 g (1 g/mm) was applied to each ring. After an equilibration period of 60 min, the rings were contracted with either 90 mM KCl or 10 μM phenylephrine until reproducible responses to each stimulus were obtained. The absence of a functional endothelium was confirmed by the lack of carbachol-induced relaxation of rings precontracted with phenylephrine.

Ritanserin vasoactivity was assessed on rings either depolarized with 90 mM KCl or stimulated with 100 nM Bay K 8644 in the presence of 20 mM KCl. A concentration-relaxation curve for ritanserin was subsequently constructed. Muscle tension was evaluated as a percent of the initial response to 90 mM KCl or Bay K 8644, which was taken as 100%. A high KCl concentration was achieved by directly adding KCl from a 2.4 M stock solution, to the organ bath solution, as neither efficacy nor potency of vasodilators is significantly affected by the resultant increase in the osmolarity compared to preparations in which the osmolarity is preserved [30].

Chemicals
The chemicals used included collagenase (type XI), trypsin inhibitor, bovine serum albumin, TEA chloride, HEPES, taurine, (S)-(-)-methyl-1,4-dihydro-2,6-dimethyl-3-nitro-4-(2-trifluoro-methylphenyl)pyridine-5-carboxylate (Bay K 8644), phenylephrine, ritanserin, and nifedipine (Sigma Chimica, Milan, Italy); ketanserin [Janssen, CEVA Logistics Italia Srl, Stradella (PV), Italy]. Bay K 8644 and nifedipine, dissolved directly in ethanol, and ritanserin, dissolved directly in DMSO, were diluted at least 1000 times prior to use. Control experiments confirmed that no response was induced in vascular preparations when DMSO or ethanol at the final concentration used in the above dilutions (0.1%, v/v) was added alone (data not shown). Final drug concentrations are stated in the text.

Statistical analysis
Acquisition and analysis of the data were accomplished using pClamp 9.2.1.9 software (Molecular Devices Corporation, Sunnyvale, CA, USA) and GraphPad Prism version 5.04 (GraphPad Software Inc., San Diego, CA, USA).

Data are reported as the mean ± SEM; n is the number of cells/rings analyzed isolated from at least three animals. Statistical analyses and significance, as measured by Student's t-test for either paired or unpaired samples (two-tailed) and repeated measures ANOVA followed by Dunnett's or Bonferroni's posttest, were obtained using GraphPad Prism version 5.04. Posttests were performed only when ANOVA found a significant value of F and no variance in homogeneity. In all comparisons, $P < 0.05$ was considered significant. The pharmacological response to ritanserin, described in terms of pIC$_{50}$ (the −log of the IC$_{50}$ value, i.e., the drug concentration reducing the response by 50%), was obtained by nonlinear regression analysis.

Docking simulations
The homology 3D model of the Ca$_V$1.2 channel pore domain was utilized as previously described [31]. Docking of the ligands ritanserin, ketanserin, and Bay K 8644 was simulated by a flexible side chain protocol with AutoDock VinaXB [32]. The ritanserin,

ketanserin, and Bay K 8644 structures were downloaded from the PubChem database in sdf format (PubChem CID 5074, 3822, and 6603728, respectively) [33], while the pdbqt file was created by using AutoDock Vina v. 1.1.2 tools [34]. Multiple ligand–protein interaction maps were generated using the Protein–Ligand Interaction Profiler (PLIP) [35]. PyMOL was used as the molecular graphics system (The PyMOL Molecular Graphics System, Version 1.8 Schrödinger, LLC.).

RESULTS

Effect of ritanserin and ketanserin on $I_{Ca1.2}$
This series of experiments were carried out to evaluate the effect of ritanserin and ketanserin (Fig. 1a) on $I_{Ca1.2}$. Figure 1b shows recordings of the inward current elicited with a clamp pulse to 10 mV from a V_h of −80 mV under control conditions and after the addition of cumulative concentrations of ritanserin, which inhibited peak $I_{Ca1.2}$ in a concentration-dependent manner with a pIC$_{50}$ (M) value of 5.47 ± 0.08 ($n = 5$; Fig. 1c). In contrast, ketanserin-induced inhibition of current amplitude was
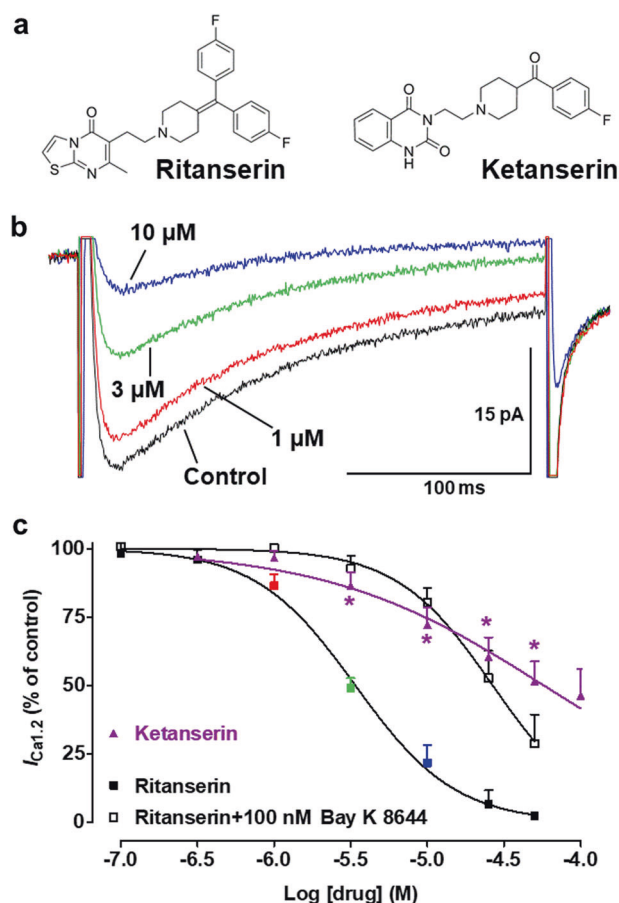
Fig. 1 Effects of ritanserin and ketanserin on $I_{Ca1.2}$ in single vascular myocytes. **a** Structure of ritanserin (left) and ketanserin (right). **b** Average traces (recorded from five cells) of $I_{Ca1.2}$, elicited with 250 ms clamp pulses to 10 mV from a V_h of −80 mV, measured in the absence (control) or presence of cumulative concentrations of ritanserin. **c** Concentration-dependent effect of ritanserin measured in the absence (control) and presence of 100 nM Bay K 8644. The concentration-response curve of ketanserin is also shown. On the ordinate scale, the current amplitude is reported as a percentage of the value recorded just before the addition of the first concentration of ritanserin or ketanserin. The curves show the best fit of the points. Data points are the mean ± SEM ($n = 5$–6). *$P < 0.05$ vs. ritanserin, Student's t test for unpaired samples

Ritanserin blocks the vascular Ca$_V$1.2 channel
F Fusi et al.

1161
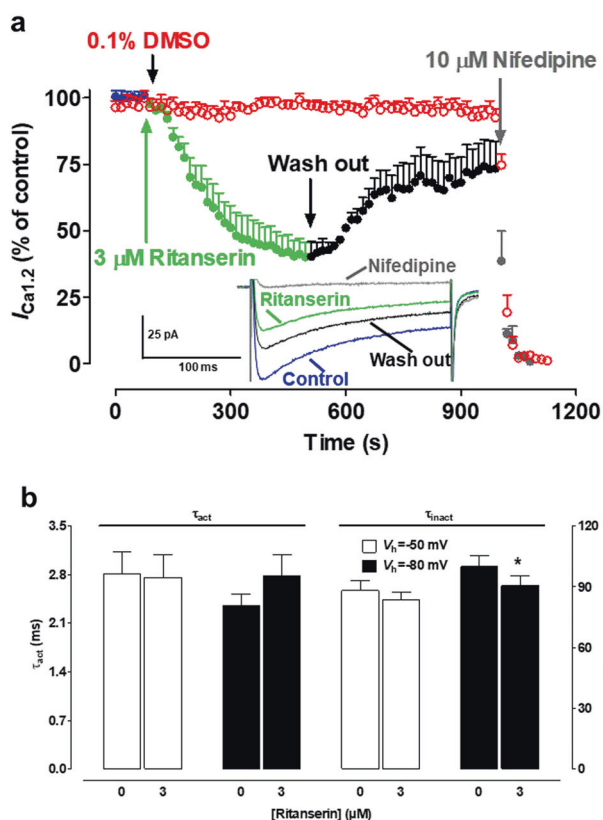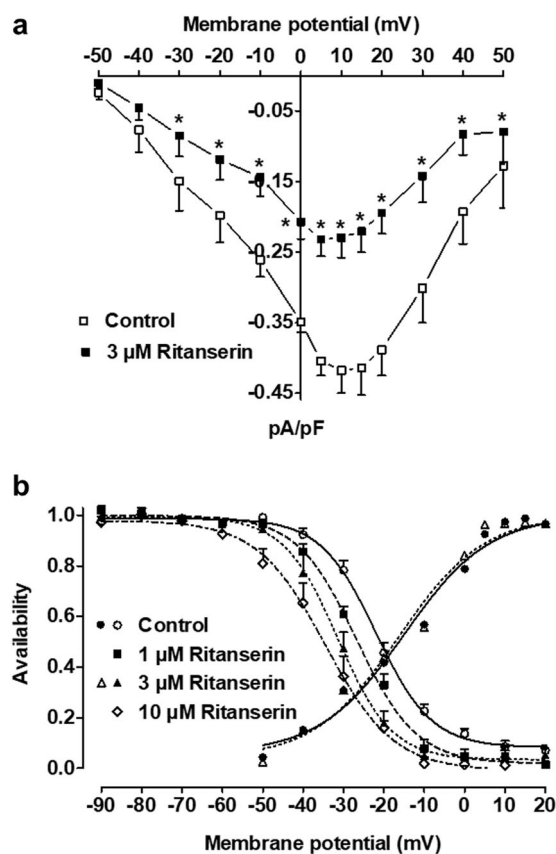

Fig. 2 Time course, washout and effect of ritanserin on the $I_{Ca1.2}$ kinetics of single vascular myocytes. **a** Time course of $I_{Ca1.2}$ inhibition induced by 3 µM ritanserin. The drug was applied at the time indicated by the arrow, and peak currents were recorded during a typical depolarization from −50 to 10 mV, applied every 15 s (0.067 Hz) and subsequently normalized according to the current recorded just prior to ritanserin addition. Drug washout gave rise to a partial recovery from the inhibition, while 10 µM nifedipine suppressed $I_{Ca1.2}$. The effect of vehicle (0.1% DMSO) is also shown. Data points are the mean ± SEM ($n = 5$–8). Inset: average traces (recorded from five cells) of $I_{Ca1.2}$ measured in the absence (control) or presence of 3 µM ritanserin, as well as after drug washout. The effect of 10 µM nifedipine is also shown. **b** Time constant for activation (τ_{act}) and inactivation (τ_{inact}) measured in the absence or presence of 3 µM ritanserin from a V_h of either −50 mV ($n = 5$) or −80 mV ($n = 10$). Columns represent the mean ± SEM. *$P = 0.0436$ vs. control, Student's t test for paired samples


Fig. 3 Voltage-dependency of ritanserin-induced inhibition of $I_{Ca1.2}$ in single vascular myocytes. **a** Current–voltage relationships, recorded from a V_h of −80 mV, constructed prior to the addition (control) and in the presence of 3 µM ritanserin. Data points are the mean ± SEM ($n = 5$). *$P < 0.05$ vs. control, Student's t test for paired samples. **b** Effect of ritanserin on the voltage dependence of Ca$_V$1.2 channel activation and inactivation. Steady-state inactivation curves, recorded from a V_h of −80 mV in the absence (control) or presence of various concentrations of ritanserin, were fitted to the Boltzmann equation. Peak current values were used. The current measured during the test pulse is plotted against the membrane potential and is expressed as availability. Steady-state activation curves were obtained from the current–voltage relationships of **a** and fitted to the Boltzmann equation. Data points are the mean ± SEM ($n = 5$)

significantly lower than that of its analog ritanserin and, at the maximal concentration assessed (100 µM), ketanserin inhibited the current amplitude by only ~50%.

To investigate whether the dihydropyridine-binding site on the channel protein was involved in the Ca^{2+} antagonistic activity of ritanserin, the potential functional interaction of ritanserin and the Ca$_V$1.2 channel stimulator Bay K 8644 was assessed. In myocytes challenged with 100 nM Bay K 8644, $I_{Ca1.2}$ increased to 524% ± 36% of the control ($n = 5$). As shown in Fig. 1c, pretreatment with Bay K 8644 caused a significant rightward shift of the ritanserin concentration-response curve (pIC$_{50}$ (M) value of 4.57 ± 0.13, $n = 5$; $P = 0.0003$ vs. control).

Characterization of the effects of ritanserin on $I_{Ca1.2}$
A biophysical and pharmacological analysis was carried out to clarify the mechanism underlying the ritanserin-induced inhibition of $I_{Ca1.2}$ and its activity was described at the channel protein. Figure 2a illustrates the time course of the effects of 3 µM ritanserin or vehicle (0.1% DMSO) on the current recorded at 0.067 Hz from a V_h of −50 mV to a test potential of 10 mV. After

$I_{Ca1.2}$ reached steady values, the addition of ritanserin to the bath solution produced a gradual decrease in the current amplitude that reached a plateau in ~5 min. In contrast, DMSO had no effect on the current amplitude. Ritanserin-induced inhibition of $I_{Ca1.2}$ was partially reversed upon drug washout (Fig. 2a) and was not affected by the membrane potential. In fact, when V_h was shifted to −80 mV, the residual current amplitude (47.2% ± 3.5% of control, $n = 5$) was similar to that recorded at a V_h of −50 mV (45.5% ± 8.6% of control, $n = 5$; $P = 0.6999$).

$I_{Ca1.2}$ evoked at 10 mV from a V_h of either −50 or −80 mV was activated and then declined with a time course that could be fitted by a monoexponential function. Ritanserin (3 µM) significantly accelerated only the τ of inactivation recorded at a V_h of −80 mV (Fig. 2b).

The current–voltage relationship (Fig. 3a) shows that 3 µM ritanserin significantly decreased the peak inward current in the range of membrane potential values from −30 to 50 mV, shifting the apparent maximum by 5 mV in the hyperpolarizing direction without varying the threshold at approximately −40 mV.

The voltage dependence of ritanserin inhibition was further investigated by analyzing the steady-state inactivation and

Ritanserin blocks the vascular Ca$_V$1.2 channel
F Fusi et al.

1162
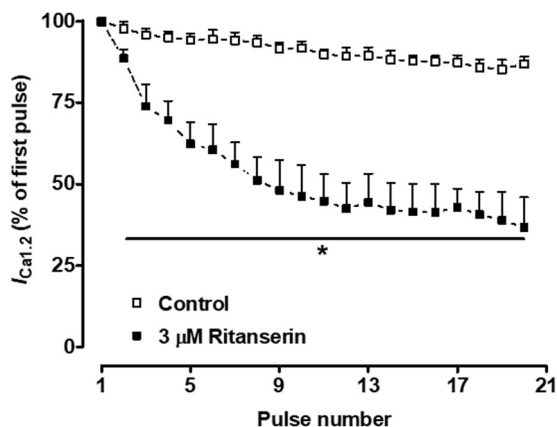
Fig. 4 Effect of ritanserin on the frequency dependence of $I_{Ca1.2}$ in single vascular myocytes. In the absence of ritanserin, 20 depolarizing 50 ms clamp pulses to 10 mV from V_h of -50 mV were applied at 1 Hz. Ritanserin (3 μM) was added just after the delivery of the first train of pulses; 4 min later, the same protocol was repeated. The peak amplitude elicited by the first train pulse (in either the absence or presence of ritanserin) was taken as 100% to better appreciate the frequency-dependent block of $I_{Ca1.2}$. Data points are the mean ± SEM ($n = 5$). *$P < 0.05$ vs. the time-matched control, Student's t test for paired samples

Fig. 5 Surface-cartoon representation of the homology model of the Ca$_V$1.2 structure. Domains I–IV are colored yellow, gray, pink, and green, respectively. Ritanserin (blue sticks), ketanserin (orange sticks), and Bay K 8644 (red sticks) are posed inside their binding pockets

activation curves for $I_{Ca1.2}$. The steady-state activation curves (Fig. 3b), calculated from the current–voltage relationships shown in Fig. 3a, were fitted with the Boltzmann equation. Ritanserin neither shifted the 50% activation potential (-17.0 ± 5.1 mV for the control, and -17.1 ± 4.5 mV for 3 μM ritanserin, $n = 5$; $P = 0.8818$, Student's t test for paired samples) nor affected the slope factor (10.3 ± 1.0 and 9.9 ± 1.0 mV, respectively; $P = 0.0865$).

The apparent dissociation constant of ritanserin for inactivated channels (K_i) was determined by the shift of Ca$_V$1.2 channel steady-state availability as a function of ritanserin concentration at a V_h of -80 mV [36]. Ritanserin significantly shifted the steady-state inactivation curve to more hyperpolarizing potentials in a concentration-dependent manner (Fig. 3b; $P = 0.0003$, repeated measures ANOVA). The 50% inactivation potential changed from -22.5 ± 1.1 mV ($n = 5$, control) to -27.2 ± 0.9 mV (1 μM ritanserin, $P > 0.05$), -31.5 ± 2.2 mV (3 μM ritanserin, $P < 0.05$), and -35.6 ± 2.7 mV (10 μM ritanserin, $P < 0.05$, Dunnett's posttest). The slope factor, however, was not affected by ritanserin (-7.2 ± 0.6, -7.1 ± 1.0, -6.3 ± 0.6, and -8.5 ± 1.1 mV, respectively; $P > 0.05$). The K_i was estimated by plotting the 50% inactivation potentials as a function of ritanserin concentration. This relationship was fitted to the equation

$$V_{50} = K_{control} \times \ln\{1/[1 + ([drug]/K_i)]\} + V_{50\,control}$$

where $V_{50\,control}$ and $K_{control}$ are the values of the 50% inactivation potential and the slope measured under control conditions, respectively. The value of K_i thus determined was 1.6 ± 0.9 μM ($n = 5$), which was not significantly different from the K_r reported above (3.6 ± 0.7 μM, $n = 5$; $P = 0.1201$, Student's t test for unpaired samples).

The shift of the inactivation curve caused by 3 μM ritanserin led to a marked reduction in the Ca^{2+} window current that peaked at approximately -20 mV (with a relative amplitude of 0.11) compared with the peak at approximately -25 mV (relative amplitude 0.19) observed under control conditions.

To assess whether ritanserin inhibition of $I_{Ca1.2}$ was frequency-dependent, the current was recorded during 20 depolarizing pulses 50 ms in length to 10 mV from a V_h of -50 mV applied at a stimulation frequency of 1 Hz. Ritanserin, at a concentration of 3 μM, produced a frequency-dependent block of $I_{Ca1.2}$ (Fig. 4). This
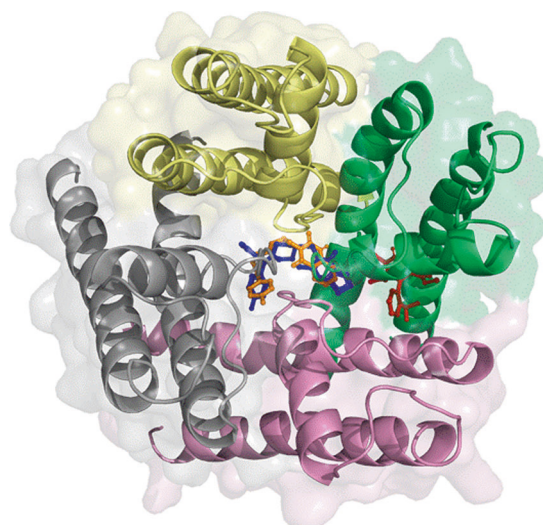
frequency dependence, calculated by normalizing the current amplitude evoked by the 20th applied stimulus against that induced by the first step pulse, was significantly greater than that observed under control conditions.

Molecular docking simulation
In silico docking was carried out to define the interaction of ritanserin with the rat Ca$_V$1.2 channel α$_{1C}$ subunit. The lowest energy poses of ritanserin, ketanserin, and Bay K 8644 showed Gibbs free-energy values (ΔG) of -8.7, -8.6, and -8.4 kcal·mol^{-1}, respectively. The computational analysis established that the three compounds were placed in the same binding region, though in different binding pockets (Fig. 5). In particular, ritanserin and ketanserin bound to the same site with good superposition; however, differences in their structure gave rise to different residue interaction networks. PLIP analysis indicated that ritanserin formed hydrophobic interactions with Leu-427, Val-430, Leu-775, and Phe-1489, a hydrogen bond with Tyr-1489, a π-stacking interaction with Phe-1190, and halogen bonds with Thr-391 and Ile-1497 (Fig. 6a), whereas ketanserin formed hydrophobic interactions with Leu-427, Met-1186, Tyr-1489, Ile-1497, Phe-1500, a π-stacking interaction with Phe-1190, and a halogen bond with Thr-1443. Conversely, Bay K 8644 gave rise to hydrophobic interactions with Thr-1066, Phe-1070, Phe-1483, and Ile-1486, and formed a strong hydrogen bond with Tyr-1489 (Fig. 6b).

The ligand–protein interaction networks showed that the orientation of Tyr-1489 present in the binding pockets accommodating either Bay K 8644 or ritanserin plays a key role in the binding of the latter to the Ca$_V$1.2 channel α$_{1C}$ subunit. Only the Tyr-1489 orientation shown in Fig. 6c was able to form a stable 3.8 Å-long hydrogen bond with ritanserin; in contrast, the Tyr-1489 orientation shown in Fig. 6d, which gave rise to the formation of a stronger 2.3 Å long hydrogen bond with Bay K 8644, was favored by the presence of Bay K 8644 in the pocket.

Effect of ritanserin on freshly isolated rat caudal artery myocytes
The contractile effect of ritanserin was evaluated by recording the morphological changes of freshly isolated cells (shortening with formation of membranous evaginations; see ref. [37]). As shown in Fig. 7a, under the experimental conditions used for patch-clamp recordings, i.e., in the presence of 5 mM Ca^{2+} and 30 mM TEA, the addition of ritanserin in the range concentration of 25–50 μM

Ritanserin blocks the vascular Ca$_V$1.2 channel
F Fusi et al.

1163
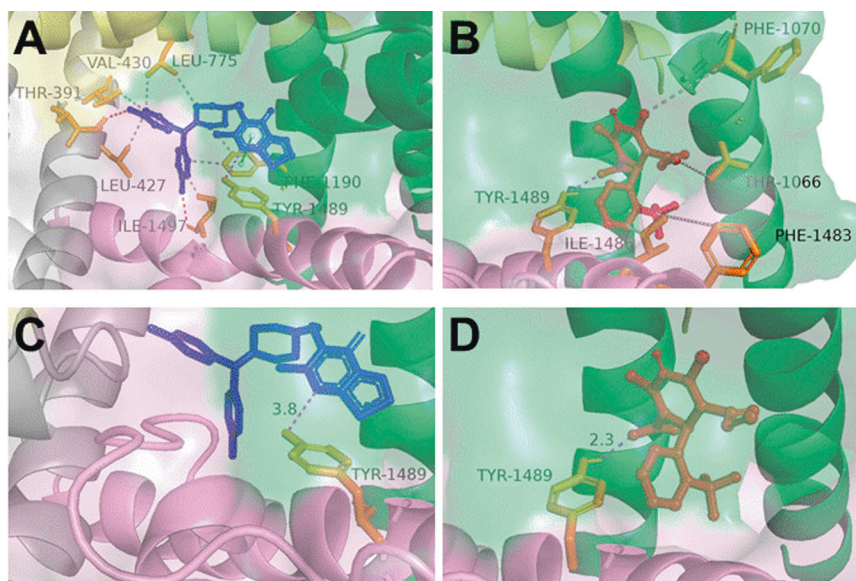
Fig. 6 Docking of ritanserin and Bay K 8644 into the Ca$_V$1.2 channel α$_{1C}$ subunit. View of **a** ritanserin and **b** Bay K 8644 (blue and red sticks, respectively) interacting with the binding pocket residues (orange sticks). The hydrogen bonds, hydrophobic interactions, and π-stacking are displayed as purple, gray, and green dotted lines, respectively. **c, d** Enlarged view showing the role played by the Tyr-1489 residue (orange sticks) in the binding of **c** ritanserin and **d** Bay K 8644. The hydrogen bond is displayed as a purple dotted line

caused cell contraction. TEA did not evoke any evident contraction per se, which is in line with what was previously observed with 60 mM K$^+$ [24]. Conversely, the addition of ritanserin did not elicit contractions in cells dialyzed under the whole-cell configuration. Similar results were obtained under the experimental conditions used for functional experiments (i.e., 2.7 mM Ca^{2+} and no TEA in the bath; Fig. 7b). Superfusion with the sole vehicle, i.e., 0.1% DMSO, did not affect the length of the myocytes (56.6 ± 6.8 μm, control; 54.7 ± 6.3 μm, 0.1% DMSO 5 min; 53.2 ± 6.0 μm, 0.1% DMSO 10 min; $P > 0.05$); however, it shortened significantly upon the addition of 0.5 mM ATP (39.6 ± 3.7 μm, $n = 7$; $P < 0.05$).

Effects of ritanserin and ketanserin on vascular rings
In rat caudal artery rings, the addition of cumulative concentrations of ritanserin did not evoke an increase in basal tone (data not shown). In preparations precontracted with 90 mM KCl (1364 ± 101 mg, $n = 13$), ritanserin induced a concentration-dependent relaxation with a pIC$_{50}$ (M) value of 5.42 ± 0.04 ($n = 13$) and a maximal inhibitory effect of 91.9% ± 3.3% ($n = 4$) (Fig. 8a, b). Ketanserin was less effective than ritanserin on 90 mM KCl-contracted rings (1219 ± 158 mg, $n = 4$), causing a relaxation of 67.9% ± 4.6% ($n = 3$; $P = 0.0149$). Drug washout for ~30–60 min caused a partial recovery of the 10 μM phenylephrine-induced contraction, which amounted to 42.1% ± 4.7% of the control (ritanserin; $n = 10$) and 76.1% ± 0.7% of the control (ketanserin; $n = 3$; $P = 0.0028$). Noticeably, 90 mM KCl-induced contraction recovered to only 10.7% ± 1.2% of the control ($n = 10$) following a 10–45 min washout of ritanserin ($P < 0.0001$ vs. phenylephrine).

Ritanserin concentration-dependently relaxed rings precontracted by 100 nM Bay K 8644 (785 ± 106 mg, $n = 7$); however, the pIC$_{50}$ (M) value was lower than that recorded in the depolarized preparations (4.66 ± 0.14, $n = 7$; $P < 0.0001$).

DISCUSSION

The present investigation provides the first direct electrophysiological evidence that ritanserin is a vascular Ca$_V$1.2 channel blocker, as demonstrated by the inhibitory effect produced by the drug on $I_{Ca1.2}$. The major findings supporting this conclusion are as follows: (1) in single vascular myocytes, ritanserin inhibited $I_{Ca1.2}$ in

a concentration-dependent manner; (2) this inhibition was antagonized by the Ca$_V$1.2 stimulator Bay K 8644 and was likely due to the interaction of ritanserin with the channel protein; (3) ritanserin stabilized the Ca$_V$1.2 channel in its inactivated state; and (4) since ritanserin relaxed vascular smooth muscle contraction resulting from the opening of Ca$_V$1.2 channels, the $I_{Ca1.2}$ blockade is supposed to have functional relevance and supports previous data obtained in vascular and nonvascular tissues [15–17], where such mechanism of action was hypothesized to account for the relaxant effects of the drug.

The potency of ritanserin was diminished when Ca$_V$1.2 channels were stimulated by Bay K 8644, in analogy with what was observed with nifedipine and Bay K 8644, which are both dihydropyridines and share the same binding site on Ca$_V$1.2 channel α$_{1C}$ subunit [38]. This observation provides compelling evidence for a mutual interaction of ritanserin and Bay K 8644 at the channel protein. The rightward shift of the ritanserin inhibition curve by Bay K 8644 might be because Bay K 8644 and ritanserin bind to channel receptor sites that are in close proximity to each other or are allosterically linked [39]. Support for this hypothesis is aroused from the in silico analysis (see below).

Ritanserin-induced inhibition of $I_{Ca1.2}$ observed at 0.067 Hz—a frequency that allows full recovery between pulses from Ca$_V$1.2 channel inactivation in rat tail artery myocytes [40]—was tonic in nature and developed independently of channel activation [41]. This is interpreted as a consequence of the selective inhibition of the resting channel state. Furthermore, ritanserin, like verapamil [42], inhibited $I_{Ca1.2}$ in a frequency-dependent fashion (use-dependent block), and similarly to nicardipine [43] shifted the channel availability toward more hyperpolarizing potentials. These effects are conventionally interpreted as a consequence of a high affinity drug binding and stabilization of inactivated channels [43]. This phenomenon, however, was not voltage-dependent. In fact, the ritanserin apparent dissociation constant for the inactivated channel (K_i) was not significantly different from that for the closed channel (K_r). This hypothesis is further supported by the similar current inhibition recorded at V_h values of −50 and −80 mV. Stabilization of the inactivated state, however, seemed to follow a slow kinetics, since the $I_{Ca1.2}$ inactivation, observed during the 250 ms long depolarizing step, was slightly affected by ritanserin

Ritanserin blocks the vascular Ca$_V$1.2 channel
F Fusi et al.

1164
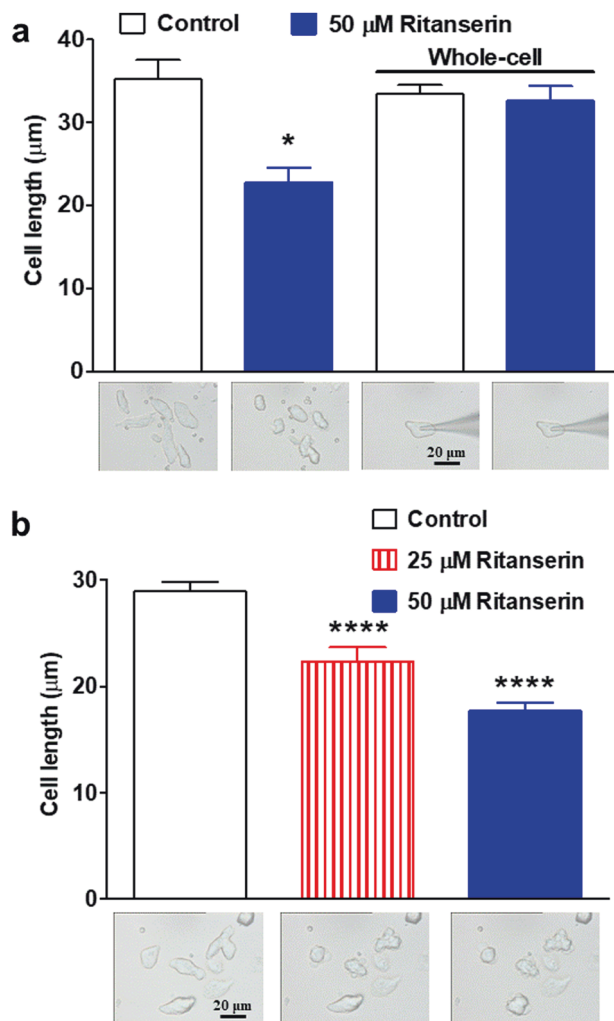
Fig. 7 Ritanserin-induced contractility of single vascular myocytes. Cell length measured before (control) and after the addition of various concentrations of ritanserin. Myocyte shortening recorded in the presence of **a** 5 mM Ca^{2+} and 30 mM tetraethylammonium or **b** 2.7 mM Ca^{2+} in the bath solution. Representative video images, taken at least one minute after treatment with the drug, are shown below each column. Only one scale bar is shown for each row. Columns are the mean ± SEM ($n = 4–16$). **a** *$P = 0.0002$ vs. control, Student's t test for paired samples; **b** ****$P < 0.0001$ repeated measures ANOVA and Dunnett's posttest

only at a V_h of −80 mV. Finally, it is conceivable that ritanserin could cause Ca$_V$1.2 channel inactivation by increasing basal cytoplasmic Ca^{2+} levels. However, this hypothesis can be ruled out, as the drug did not increase the resting smooth muscle tone of artery rings when added to the organ bath in the absence of other stimulating agents. Taken together, these findings indicate that within the frame of the "state-dependent pharmacology" of the channel, three different mechanisms, operated simultaneously by ritanserin, are responsible for Ca$_V$1.2 channel block: state-independent (tonic), weak state-dependent open channel inhibition (the faster Ca$_V$1.2 channel inactivation kinetics observed in the presence of the drug, reported also for other Ca$_V$1.2 channel blockers such as dihydropyridines and phenylalkylamines) [42], and state-dependent inactivated channel stabilization.

The leftward shift of the steady-state inactivation curve operated by ritanserin, caused a marked reduction of the window current. This current is physiologically relevant because is thought to be largely responsible for both generation and regulation of vascular smooth muscle tone [44]. Therefore, when preincubated
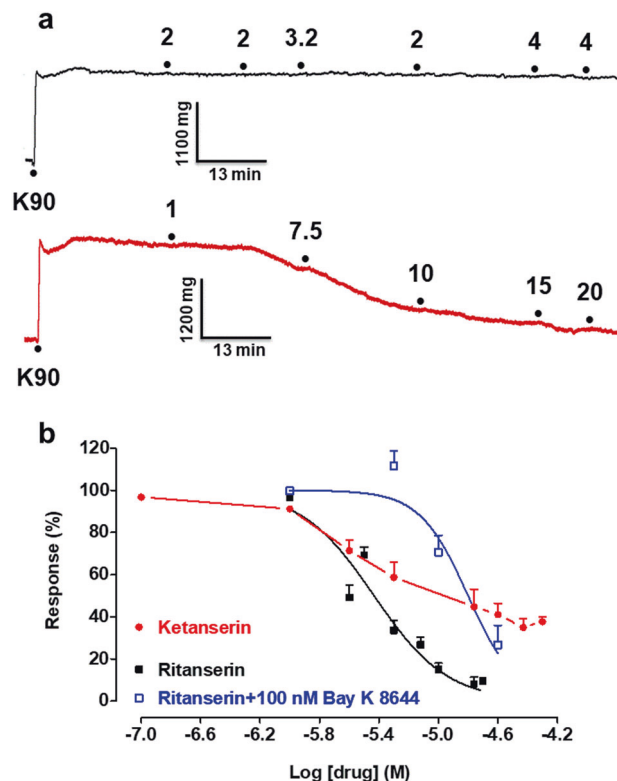
Fig. 8 Effects of ritanserin and ketanserin on rat tail artery rings. **a** Original recordings of isometric tension (representative of 13 similar experiments) of the relaxation caused by cumulative concentrations of ritanserin (μM) added (lower trace) at the plateau of 90 mM K$^+$ (K90)-induced contraction in rat tail artery rings. The effect of vehicle (DMSO, in μL) is also shown (upper trace). **b** Concentration–response curves of the relaxing effect of ritanserin and ketanserin on rings precontracted by either 100 nM Bay K 8644 (only ritanserin) or 90 mM KCl. Bay K 8644-induced contractile response was obtained following pretreatment of the ring with 20 mM KCl. On the ordinate scale, the response is reported as a percent of the tension induced by the contracting agent (100%). Data points are the mean ± SEM ($n = 3–7$)

in vitro with the isolated preparations, ritanserin may cause relaxation per se via a reduction of the window current. On the other hand, although ritanserin shifted the voltage at which the maximum of the current–voltage relationship occurred by 5 mV, neither the slope nor the 50% activation potential were affected by the drug, thus indicating that the sensitivity of the channel activation mechanism to the membrane voltage was only modestly altered.

Docking results demonstrated that, similar to dihydropyridine Ca$_V$1.2 channel blockers [45], ritanserin bound to the outer, lipid-facing surface of the pore in the intersubunit crevice formed by neighboring tilted S5–S6 helices and the P-loop of domains III and IV, a region involved in Ca$_V$1.2 inactivation [46, 47]. Noticeably, ritanserin and Bay K 8644 bound to the same region, though to different, very closely situated pockets, analogous to what was previously observed with the PKA inhibitor H-89 [48]. The Tyr-1489 residue, located in the overlapping area, was crucial for the interaction of the two molecules with the channel protein. The conformation of the residue shown in Fig. 6c allowed ritanserin binding. Conversely, when the residue assumed the conformation shown in Fig. 6d only Bay K 8644 was able to dock. Additionally, the Tyr-1489 residue conformation is important in shaping the channel pore state [46, 47] indicating that the conformation favored by ritanserin stabilizes the closed state, while that favored by Bay K 8644 stabilizes the open state of the channel. Finally, the

Ritanserin blocks the vascular Ca$_V$1.2 channel
F Fusi et al.

1165

two different docking poses and hydrogen bond lengths likely explain the decreased Ca^{2+} antagonist potency of ritanserin recorded in the presence of Bay K 8644. The lower inhibitory effect of ketanserin compared to ritanserin could be due to its different interaction network with binding pocket residues and, in particular, to the lack of interaction with the key Tyr-1489 residue.

Ritanserin inhibited $I_{Ca1.2}$ in the same cells where it induced a contractile effect. Noticeably, dialysis of the cytoplasm (as in the case of the conventional whole-cell method) prevented cell contraction but not inhibition of $I_{Ca1.2}$. This observation suggests that contraction was mediated by a rise in cytoplasmic Ca^{2+} concentration (which, in the whole-cell configuration, is buffered by the high level of EGTA present in the pipette solution) and/or by diffusible intracellular factors. On the other hand, ritanserin inhibition of $I_{Ca1.2}$ seems to be related to a direct interaction of the drug with the channel protein, although the possible involvement of intracellular signaling pathways surviving dialysis cannot be ruled out. Taken together, these results indicate that the drug is able to activate both vasoconstricting and vasorelaxant mechanisms, the former prevailing in single cells and the latter in intact tissue either in resting conditions or under the presence of stimulating agents such as high concentrations of K$^+$. This apparent discrepancy, previously observed with the rat toxicant norbormide [49] and described with high K$^+$ [24] likely follows the disruption of the extracellular matrix and ensuing isolation of single smooth muscle cells, leading to the loss of focal contact tension that in turn considerably alters cell signaling systems [50]. Moreover, this hypothesis argues that the relaxation effect elicited by ritanserin in the intact tissue may be underestimated, i.e., inhibition of the Ca$_V$1.2 channel by itself would induce a more pronounced vasorelaxation.

Ca$_V$1.2 channel inhibition was also observed in intact tissue under conditions of full membrane depolarization, i.e., in vascular rings depolarized with high K$^+$ concentrations. Under experimental conditions similar to those represented by voltage-clamp pulses of depolarization applied to evoke $I_{Ca1.2}$ ritanserin caused relaxation and its potency and efficacy were consistent with those calculated in the patch-clamp experiments. Furthermore, this vasorelaxant effect was significantly antagonized by the Ca$_V$1.2 channel agonist Bay K 8644, which is in perfect agreement with what was observed in single myocytes, thus supporting the hypothesis of a mutual interaction of ritanserin and Bay K 8644 at the channel protein. Finally, in rat caudal artery rings, the myorelaxant effect of the drug was only partially reverted by washout, similar to what was observed in the patch-clamp experiments. The partial reversibility of ritanserin $I_{Ca1.2}$ antagonism observed in the present study suggested a relatively strong interaction of the drug with the channel protein. In fact, recovery of high K$^+$-induced contraction (essentially dependent on the opening of Ca$_V$1.2 channels) was significantly lower than that correlated to phenylephrine (only partly dependent on the opening of Ca$_V$1.2 channels). Furthermore, this effect was similar to that previously reported in isolated dog cardiac tissue [6], where the effects of ritanserin could not be fully reversed even after 2 h of repeated washout with physiological solution.

Interestingly, ketanserin, when assessed on both smooth muscle active tone and $I_{Ca1.2}$ amplitude, showed a much lower activity compared to its analog ritanserin. In silico docking and postdocking analyses, displaying a higher number and stronger type of interactions toward the binding pocket for ritanserin compared to ketanserin, well supported these experimental observations. Taken together, these data strengthen the hypothesis of the existence of a rather specific ritanserin structure–Ca$_V$1.2 channel blocking activity relationship.

In conclusion, the present electrophysiological, functional, and in silico data point to ritanserin as a vasorelaxant and Ca$_V$1.2 channel blocking agent. This observation may open a new avenue for the treatment of Raynaud's syndrome. In this disorder, either

Ca$_V$1.2 channel blockers, such as nifedipine [21], or 5-HT$_2$ receptor antagonists, such as sarpogrelate [18–20], are effective therapeutic agents. Therefore, the Ca$_V$1.2 channel and 5-HT$_2$ receptor antagonist ritanserin may represent an interesting scaffold to develop bifunctional defense drugs for the treatment of Raynaud's phenomenon, as opposed to ketanserin, which was previously defined as not clinically beneficial for the treatment of this disorder in progressive systemic sclerosis [51]. The discovery of a contractile pathway activated by the drug suggests that ritanserin derivatives, possibly deprived of the contractile property, would give rise to relaxing agents that are more potent than the parent compound itself. Finally, in search of effective drugs for the treatment of Reynaud's syndrome, forthcoming analysis of some 5-HT$_2$ receptor antagonists will clarify whether other agents besides ritanserin emerge as scaffolds worthy of further pharmaceutical development.

AUTHOR CONTRIBUTIONS
FF and SB designed the research; FF, AT, and SB performed the research; FF and AT analyzed the data; FF, OS, SS, and SB wrote the paper; and GS critically revised the paper.

ADDITIONAL INFORMATION

REFERENCES
1. Leysen JE, Gommeren W, Van Gompel P, Wynants J, Janssen PF, Laduron PM. Receptor-binding properties in vitro and in vivo of ritanserin: a very potent and long acting serotonin-S2 antagonist. Mol Pharmacol 1985;27:600–11.
2. https://www.guidetopharmacology.org/GRAC/LigandDisplayForward?tab=biology&ligandId=97. Accessed 9 Mar 2019.
3. Kriston L, von Wolff A, Westphal A, Hölzel LP, Härter M. Efficacy and acceptability of acute treatments for persistent depressive disorder: a network meta-analysis. Depress Anxiety 2014;31:621–30.
4. Singh SP, Singh V, Kar N, Chan K. Efficacy of antidepressants in treating the negative symptoms of chronic schizophrenia: meta-analysis [published correction appears in Br J Psychiatry. 2011;198:159]. Br J Psychiatry. 2010;197:174–9.
5. Cornish JW, Maany I, Fudala PJ, Ehrman RN, Robbins SJ, O'Brien CP. A randomized, double-blind, placebo-controlled study of ritanserin pharmacotherapy for cocaine dependence. Drug Alcohol Depend. 2001;61:183–9.
6. Wu K, Hunter TL, Proakis AG. Effects of ritanserin on transmembrane action potentials in canine purkinje fibres. Proc Soc Exp Biol Med. 1992;199:88–92.
7. Boroda S, Niccum M, Raje V, Purow BV, Harris TE. Dual activities of ritanserin and R59022 as DGKa inhibitors and serotonin receptor antagonists. Biochem Pharmacol. 2017;123:29–39.
8. Arranz-Nicolás J, Ogando J, Soutar D, Arcos-Pérez R, Meraviglia-Crivelli D, Mañes S, et al. Diacylglycerol kinase α inactivation is an integral component of the costimulatory pathway that amplifies TCR signals. Cancer Immunol Immunother. 2018;67:965–98.
9. Olmez I, Love S, Xiao A, Manigat L, Randolph P, McKenna BD, et al. Targeting the mesenchymal subtype in glioblastoma and other cancers via inhibition of diacylglycerol kinase alpha. Neuro Oncol. 2018;20:192–202.
10. Franks CE, Campbell ST, Purow BW, Harris KL. The ligand binding landscape of diacylglycerol kinases. Cell Chem Biol. 2017;24:870–80.
11. Campbell ST, Franks CE, Borne AL, Shin M, Zhang L, Hsu KL. Chemoproteomic discovery of a ritanserin-targeted kinase network mediating apoptotic cell death of lung tumor cells. Mol Pharmacol. 2018;94:1246–55.
12. Van Nueten JM, Schuurkes JAJ, De Ridder WJE, Kuyps JJMD, Janssens WJ. Comparative pharmacological profile of ritanserin and ketanserin. Drug Dev Res. 1986;8:187–95.
13. Frenken M, Kaumann AJ. Allosteric properties of the 5-HT$_2$ receptor system of the rat tail artery. Ritanserin and methysergide are not competitive 5-HT$_2$ receptor antagonists but allosteric modulators. Naunyn Schmiedebergs Arch Pharmacol. 1987;335:359–66.

14. Conolan S, Quinn MJ, Taylor DA. In vivo and in vitro activity of selective 5-hydroxytryptamine$_2$ receptor antagonists. Br J Pharmacol. 1986;89:129–35.

15. Okoro EO, Marwood JF, Stokes GS. The interaction between Ca^{2+}, verapamil and ketanserin in rat tail artery aorta. J Cardiovasc Pharmacol. 1995;25:603–10.

16. Okoro EO, Marwood JF. Effects of 5-HT$_2$ receptor antagonists on responses to potassium depolarization, in rat isolated aorta. Clin Exp Pharmacol Physiol. 1997;24:34–9.

17. Okoro EO. Overlap in the pharmacology of L-type Ca^{2+}-channel blockers and 5-HT$_2$ receptor antagonists in rat aorta. J Pharm Pharmacol. 1999;51:953–7.

18. Kumagai S, Morinobu A, Ozaki S, Nakao K, Ishida H. Sarpogrelate hydrochloride for Raynaud's phenomenon of patients with collagen diseases. Ryumachi. 1998;38:504–10.

19. Yoshimasu T, Ikeda T, Uede K, Kanazawa N, Furukawa F. Effects of sarpogrelate hydrochloride on skin ulcers and quality of life in patients with systemic sclerosis. J Dermatol. 2012;39:536–40.

20. Ogawa T, Ogura T, Hirata A, Hayashi N, Izumi Y, Morita S, et al. Sarpogrelate hydrochloride therapy for Raynaud's phenomenon in patients with systemic sclerosis. Int J Rheum Dis. 2008;11:A483.

21. Rirash F, Tingey PC, Harding SE, Maxwell LJ, Tanjong Ghogomu E, Wells GA, et al. Calcium channel blockers for primary and secondary Raynaud's phenomenon. Cochrane Database Syst Rev. 2017;12:CD000467.

22. Zamponi GW, Striessnig J, Koschak A, Dolphin AC. The physiology, pathology, and pharmacology of voltage-gated calcium channels and their future therapeutic potential. Pharmacol Rev. 2015;67:821–70.

23. Fusi F, Cavalli M, Mulholland D, Crouch NR, Coombes P, Dawson G, et al. Cardamonin is a bifunctional vasodilator that inhibits Ca$_V$1.2 current and stimulates K$_{Ca}$1.1 current in rat tail artery myocytes. J Pharmacol Exp Ther. 2010;332:531–40.

24. Mugnai P, Durante M, Sgaragli G, Saponara S, Paliuri G, Bova S, et al. L-type Ca^{2+} channel current characteristics are preserved in rat tail artery myocytes after one-day storage. Acta Physiol. 2014;211:334–45.

25. Fusi F, Sgaragli G, Saponara S. Mechanism of myricetin stimulation of vascular L-type Ca^{2+} current. J Pharmacol Exp Ther. 2005;313:790–7.

26. Petkov GV, Fusi F, Saponara S, Gagov H, Sgaragli GP, Boev KK. Characterization of voltage-gated calcium currents in freshly isolated smooth muscle cells from rat tail main artery. Acta Physiol Scand. 2001;173:257–65.

27. Karmažínová M, Lacinová Ľ. Measurement of cellular excitability by whole cell patch clamp technique. Physiol Res. 2010;59:S1–7.

28. Altura BM, Altura BT, Carella A, Turlapaty PD. Adverse effects of artificial buffers on contractile responses of arterial and venous smooth muscle. Br J Pharmacol. 1980;69:207–14.

29. Bova S, Trevisi L, Debetto P, Cima L, Furnari M, Luciani S, et al. Vasorelaxant properties of norbormide, a selective vasoconstrictor agent for the rat microvasculature. Br J Pharmacol. 1996;117:1041–6.

30. Magnon M, Calderone V, Floch A, Cavero I. Influence of depolarization on vasorelaxant potency and efficacy of Ca^{2+} entry blockers, K$^+$ channel openers, nitrate derivatives, salbutamol and papaverine in rat aortic rings. Naunyn Schmiedeberg's Arch Pharmacol. 1998;358:452–63.

31. Fusi F, Manetti F, Durante M, Sgaragli G, Saponara S. The vasodilator papaverine stimulates L-type Ca^{2+} current in rat tail artery myocytes via a PKA-dependent mechanism. Vasc Pharmacol. 2016;76:53–61.

32. Koebel MR, Schmadeke G, Posner RG, Sirimulla S. AutoDock VinaXB: implementation of XBSF, new empirical halogen bond scoring function, into AutoDock Vina. J Cheminform. 2016;8:27.

33. Kim S, Thiessen PA, Bolton EE, Chen J, Fu G, Gindulyte A, et al. PubChem substance and compound databases. Nucleic Acids Res. 2016;44:D1202–13.

34. Morris GM, Huey R, Lindstrom W, Sanner MF, Belew RK, Goodsell DS, et al. Autodock4 and AutoDockTools4: automated docking with selective receptor flexibility. J Comput Chem. 2009;16:2785–91.

35. Salentin S, Schreiber S, Haupt VJ, Adasme MF, Schroeder M. PLIP: fully automated protein–ligand interaction profiler. Nucleic Acids Res. 2015;43:W443–7.

36. Bean BP, Cohen CJ, Tsien RW. Lidocaine block of cardiac sodium channels. J Gen Physiol. 1983;81:613–42.

37. Ives HE, Schultz GS, Galardy RE, Jamieson JD. Preparation of functional smooth muscle cells from the rabbit aorta. J Exp Med. 1978;148:1400–13.

38. Saponara S, Durante M, Spiga O, Mugnai P, Sgaragli G, Huong TT, et al. Functional, electrophysiological and molecular docking analysis of the modulation of Ca$_V$1.2 channels in rat vascular myocytes by murrayafoline A. Br J Pharmacol. 2016;173:292–304.

39. Hockerman GH, Peterson BZ, Johnson BD, Catterall WA. Molecular determinants of drug binding and action on L-type calcium channels. Annu Rev Pharmacol Toxicol. 1997;37:361–96.

40. Saponara S, Sgaragli G, Fusi F. Quercetin as a novel activator of L-type Ca^{2+} channels in rat tail artery smooth muscle cells. Br J Pharmacol. 2002;135:1819–27.

41. Kuriyama H, Kitamura K, Nabata H. Pharmacological and physiological significance of ion channels and factors that modulate them in vascular tissues. Pharmacol Rev. 1995;47:387–573.

42. McDonald TF, Pelzer S, Trautwein W, Pelzer DJ. Regulation and modulation of calcium channels in cardiac, skeletal, and smooth muscle cells. Physiol Rev. 1994;74:365–507.

43. Bean BP. Nitrendipine block of cardiac calcium channels: high-affinity binding to the inactivated state. Proc Natl Acad Sci U S A. 1984;81:6388–92.

44. Fransen P, Van Hove CE, van Langen J, Schrijvers DM, Martinet W, De Meyer GR, et al. Contribution of transient and sustained calcium influx, and sensitization to depolarization-induced contractions of the intact mouse aorta. BMC Physiol. 2012;12:9.

45. Tang L, Gamal El-Din TM, Swanson TM, Pryde DC, Scheuer T, Zheng N, et al. Structural basis for inhibition of a voltage-gated Ca^{2+} channel by Ca^{2+} antagonist drugs. Nature 2016;537:117–21.

46. Tikhonov DB, Zhorov BS. Structural model for dihydropyridine binding to L-type calcium channels. J Biol Chem. 2009;284:19006–17.

47. Trezza A, Bernini A, Spiga O. Identification of "on-off residues" in rat Ca$_V$1.2 α_{1C} subunit channel using in silico analysis and docking simulation. PeerJ Prepr. 2016;4:e2272v1.

48. Fusi F, Trezza A, Spiga O, Sgaragli G, Bova S. Ca(v)1.2 channel current block by the PKA inhibitor H-89 in rat tail artery myocytes via a PKA-independent mechanism: electrophysiological, functional, and molecular docking studies. Biochem Pharmacol. 2017;140:53–63.

49. Fusi F, Saponara S, Sgaragli G, Cargnelli G, Bova S. Ca^{2+} entry blocking and contractility promoting actions of norbormide in single rat caudal artery myocytes. Br J Pharmacol. 2002;137:323–8.

50. Ratz PH, Berg KM, Urban NH, Miner AS. Regulation of smooth muscle calcium sensitivity: KCl as a calcium sensitizing stimulus. Am J Physiol Cell Physiol. 2005;288:C769–83.

51. Pope J, Fenlon D, Thompson A, Shea B, Furst D, Wells G, et al. Ketanserin for Raynaud's phenomenon in progressive systemic sclerosis. Cochrane Database Syst Rev. 2000;2:CD000954.